National Conference with International Participation
ENGINEERING MECHANICS 2003
Svratka, Czech Republic, May 12 – 15, 2003
paper no. 318

FUNDAMENTAL DYNAMIC CHARACTERISTICS OF HUMAN SKULL

J. Horáček*, L. Pešek*, J. Trnka*, J. Veselý*, E. Veselý*, M. Vohradník, J. Vokřál****

Summary: *The contribution presents experimental investigation of the frequency modal, damping and stress wave propagation characteristics and finite element (FE) modeling of the basic dynamic properties of the human skull. Original experimental results of the modal analysis (Fig. 1a) as well as the laserinterferometry and double pulse holorinterferometry measurements (Fig. 1b). after impact loading are presented. The frequency and time dependent transfer functions between selected, anthropologically important points on the skull are studied. The influence of the soft brain tissues on dynamics of the skull was approximately simulated by especially prepared gelatin. The 3D FE model of the human skull (Fig. 2) was developed from the computer tomograph (CT) images of the skull investigated experimentally. The FE model incorporates also a model of the interaction of the skull bones with the brain tissue. The developed FE model is verified by the results of the measurements of fundamental frequency-modal characteristics and the transfer functions in time and frequency domain. The FE model enables approximate modeling of the sound transmission in the human skull to hearing organs by the bone conduction in hearing frequency range.*

1. Introduction

The purpose of the study was to create a computational FE model for modelling the sound transmission in the human skull by bone conduction and to use such model in simulations of perception of the external noise and own voice of human being including the effects of various weak spots of sound transmission paths causing hearing disorders. The FE model should help in optimisation of hearing or protective aids and in design of appropriate prostheses for improvement of vibroacoustic properties of sound transmission system of a handicapped human being. A proper physically based analysis of real transmission of sound waves in the head is missing.

The perception of sound and vibrations is going via hair cells of the cochlea and vibrotactile sensations. The sound passes to the cochlea via two pathways. The first way is air conduction - via tympanic membrane. The sound is conducted through middle ear ossicules to endolympha of the inner ear. The second way is so called bone conduction. Both the sound from environment and the sound of own personal voice pass to the cochlea directly through bones of the skull. The difference of hearing level of the cochlea between bone and air perception is approximately 40 dB. The perception of the own voice is quite unknown. The difference between perception of one's voice during speech (both ways) and hearing quality from the tape recorder (the air conduction only) is just the change caused by the bone

*) Ing. Jaromír Horáček, DrSc., Ing. Luděk Pešek, CSc., Ing. Jan Trnka, CSc., Ing. Jan Veselý, Ing. Eduard Veselý, CSc., Institute of Thermomechanics, Academy of Sciences of the Czech Republic, Dolejškova 5, 182 00, Prague 8, Czech Republic
**)MUDr. Miloš Vohradník, CSc., Ing. Jan Vokřál, PhD., Phoniatric Laboratory, 1st Medical Faculty of the Charles University, Žitná 24, 120 00 Prague 2, Czech Republic

conduction. The principles of conduction of acoustic waves in the skull and intervention of soft tissues in this area are unknown.

The vibration characteristics of a human skull were studied by time average holography in (Ogura et al., 1979; Hoyer & Dörheide, 1983) where the better quality holograms were obtained only for the resonant frequencies higher than 2000 Hz. The lowest natural frequencies of the skulls *in vivo* were studied by Hakansson et al. (1994,1996), where the linearity of the sound transmission through the skull was approved. The measurement of vibration amplitudes on the forehead and on the chest during phonation of different vowels is briefly reported by Sundberg (1981). Laitakari et al. (1995) measured *in situ* the vibrations of the forehead excited by the bone-anchored hearing aid (BAHA). Similar measurement *in vitro* was performed by Stenfelt et al. (2000). The first resonant frequency of the dry skull excited by the BAHA transducer was found to be 1200 Hz. Real head measurement of the vibratory responses to the bone-conduction clicks excited by pulses from the bone vibrator at various points on the skull was performed by Durrant et al. (1993).

Studies on dynamic response of human head after a transient impact loading are usually focused on various head injury mechanisms. Head impact experiments and the brain injuries were simulated mainly by FE modelling (see, e.g., Bandak 1995; King et al. 1995). Influence of the skull-brain interface on the dynamic response of the 2D FE model of the human head after impact loading was studied by Kuijpers et al. (1995).

Recently Mišun & Přikryl (2001) and Přikryl (2001) analysed by FE modelling the sound wave propagation in the dry human skull to the hearing system centre in frequency domain. They concluded that the resonant frequencies of the skull do not have any influence on the fundamental voice frequencies up to 1.2 kHz. The harmonic excitation by a bone transducer was simulated in the frequency region 200-5 500 Hz using ANSYS FE code.

The double pulse holointerferometry was successfully applied in previous studies of Trnka & Veselý (1999) on transient dynamic response of structures in solid mechanics. In biomechanics of human head the double pulse holographic interferometry was used for visualisation of the skin vibrations near the mouth and on the neck during singing (Sundberg, 1992; Pawlowski et al. 1985).

Procedures for an automatic generation of 3D FE models of the skull, brain or the complete simplified human head from CT or MR images are described for example by Krabbel & Appel (1995), Formánek (1999) and Kršek (2000).

For reliable theoretical modelling the FE model has to approximate the fundamental dynamic properties of the system such as the natural frequencies, modes of vibration, damping and basic wave propagation characteristics. Following the previous contributions of the authors presented at various conferences this study summarises dynamic characteristics obtained by the authors in the original experiments as well as by calculations using the developed FE model of the skull. The theoretical results of the modal and transient analysis of the FE model are compared with the measurement in the time as well as frequency domain.

2. Experimental modal analysis and basic vibration properties of the skull

2.1. Measurement set-up for modal analysis

The experimental set-up for modal analysis of two male skulls (I and II) investigated is shown in Fig.1. The skull was hinging on rubber springs so that the frequency of the flexible support was two orders less than the first investigated natural frequency.

The experimental modal analysis was based on the evaluation of the frequency response functions $H(f)$ measured by B&K 2032 Dual Channel FFT Analyzer. The skull was excited by the B&K 4810 vibration exciter. The excitation force was measured by the miniature B&K 8203 force transducer and the response by the B&K 4374 miniature accelerometer. The

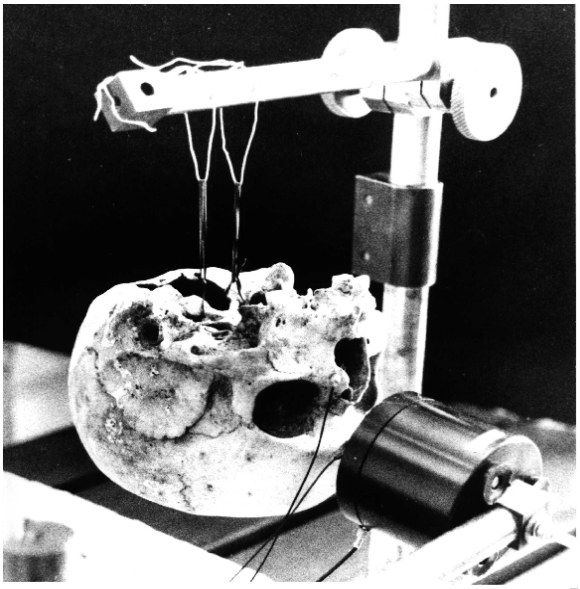

Fig. 1 Tested skull.

impact excitation was used. The frequency response functions $H(f)$ were measured at N=66 points in the frequency range 0-6.4 kHz. By smoothing these data (H_j (f)=ReH_j (f)+i ImH_j (f), j=1,2,...,N) in the complex plane, the complex eigenvalues λ=Re λ+i Im λ were evaluated and the natural frequencies f [Hz] = Im $\lambda/2\pi$, natural modes of vibration and the damping parameters D=|Re λ/Im λ| were obtained using the global method of identification (Kozánek 1995).

The frequency response functions were measured at 66 points on the skull in three planes denoted in Fig.2:

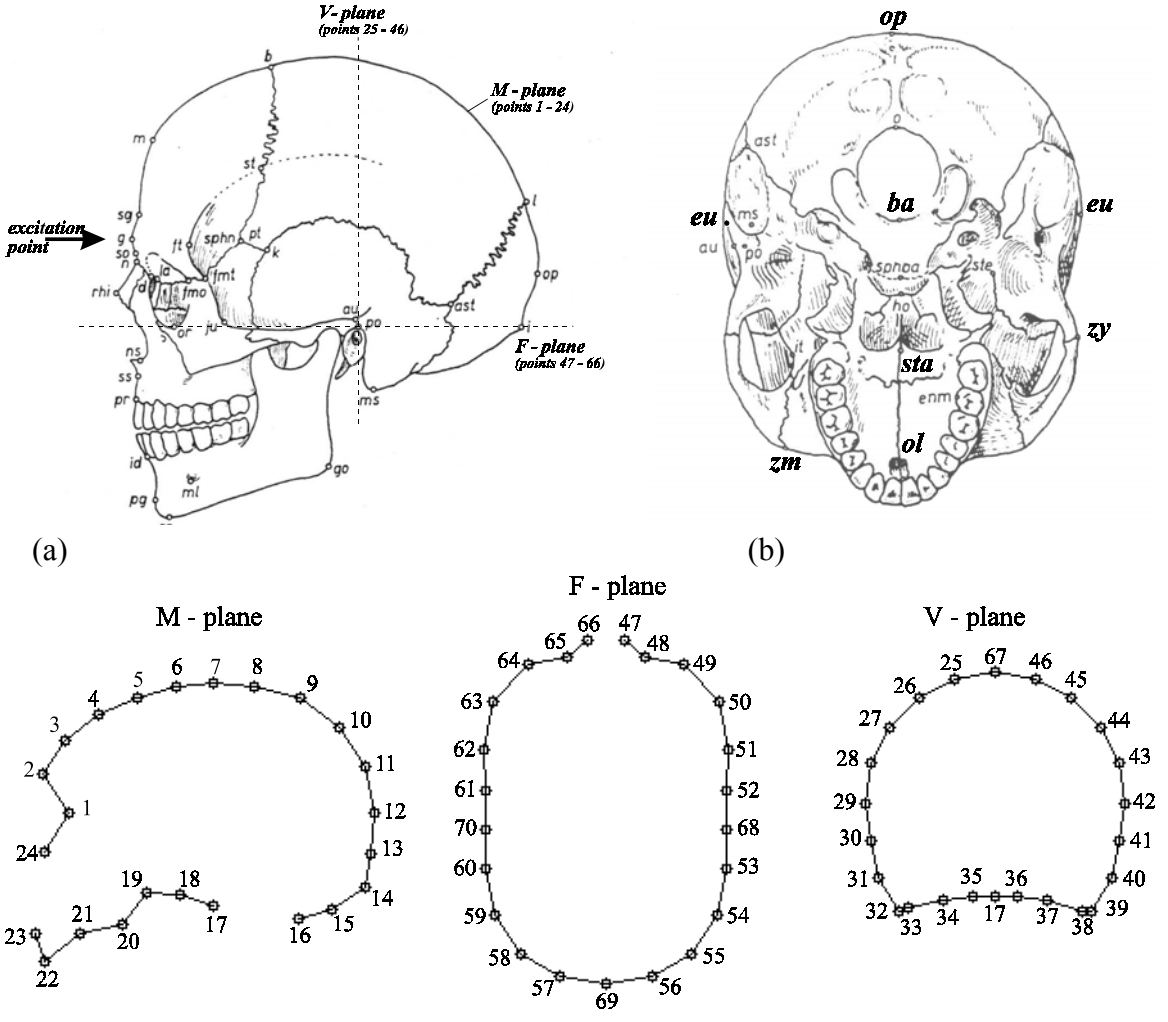

(a) (b)

(c)

Fig. 2: Excitation and measurement points on the skull.

- *M* - the median plane defined by the points: *n* (nasion), *m* (metopion) and *i* (inion),
- *F* - the horizontal so-called Frankfurt plane defined by the points: *po* (porion), *i* (inion),
- *V* - the vertical plane that is normal to the *F* - plane crossing it at the point: *po* (porion).
  The skull was excited at the point *g* (glabella) on the os frontale.

The effect of the brain soft tissues was approximately modelled by gelatine (density $\rho_f = 1030$ kg/m^3, Young's modulus $E_f \approx 12\,000$ Pa, Poisson's ratio $\mu_f \approx 0.5$). We note that for the human brain is $\rho_{br} = 1040$ kg/m^3, $E_{br} = 66700$ Pa, $\mu_{br} \approx 0.48$ - 0.499 (Kumaresan et al., 1996).

2.2. Results of the experimental modal analysis

All 66 measured functions $H_j(f)$ for the dry and non-dry skull (II) are shown in Fig. 3. The first group of the resonant frequencies for the dry skulls is between 1400 and 1700 Hz. The second region of dominant resonant frequencies is near 3000 Hz and above 4500 Hz the spectrum of the natural frequencies is very dense and due to a relatively high damping the separation of individual frequencies and mode shapes is difficult.

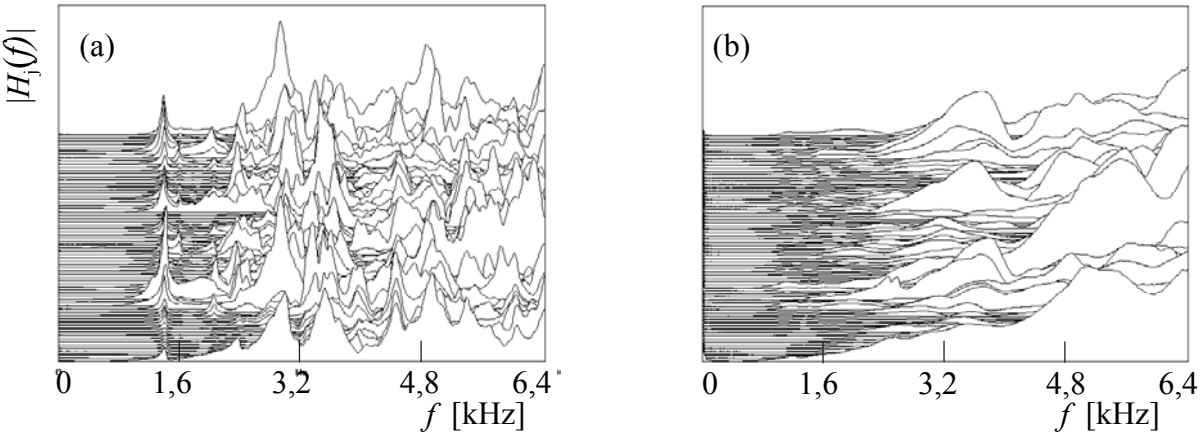

Fig. 3: Measured frequency response functions for:
a) dry skull (II), b) non-dry skull (II); ($j = 1, 2, \ldots, 66$).

	(I)		(II)	
No	f [Hz]	D [1]	f [Hz]	D [1]
1	1436	0.018	1388	0.012
2	1570	0.014	1581	0.013
3	1666	0.014	1776	0.011
4	2021	0.012	2045	0.014
5	2087	0.016	-	-
6	2194	0.019	2261	0.023
7	2241	0.012	2370	0.017
8	2440	0.023	2438	0.021
9	2557	0.023	2555	0.033
10	2676	0.018	2762	0.021

Tab. 1: Natural frequencies and damping ratios for the dry skulls.

No	f [Hz]	D [1]
1	1115	0.066
2	1243	0.077
3	1391	0.060
4	1576	0.066
5	1792	0.071
6	2039	0.089
7	2093	0.077

Tab. 2: Natural frequencies and damping ratios for the dry skull (II).

The lowest evaluated natural frequencies *f* and damping parameters *D* are summarised for both dry skulls in Tab. 1. The differences between the skulls (I) and (II) concerning the spectra of the lowest natural frequencies as well as the measured damping parameters are not significant. The measured lowest natural frequencies and damping parameters *D* of non-dry skull (II) are summarised in Tab. 2. From modelling of the soft tissues it follows that, the decrease of the fundamental natural frequencies due to the added mass of the gel is substantial as well as the increase of the damping of the system due to the viscosity of the filling. The decrease of the fundamental natural frequency for the fluid filled skull is approximately 20% in comparison with the results for the dry skull. The decrease is much smaller than 53% estimated for the human head in the study of Khalil et al. (1979) where one man and one

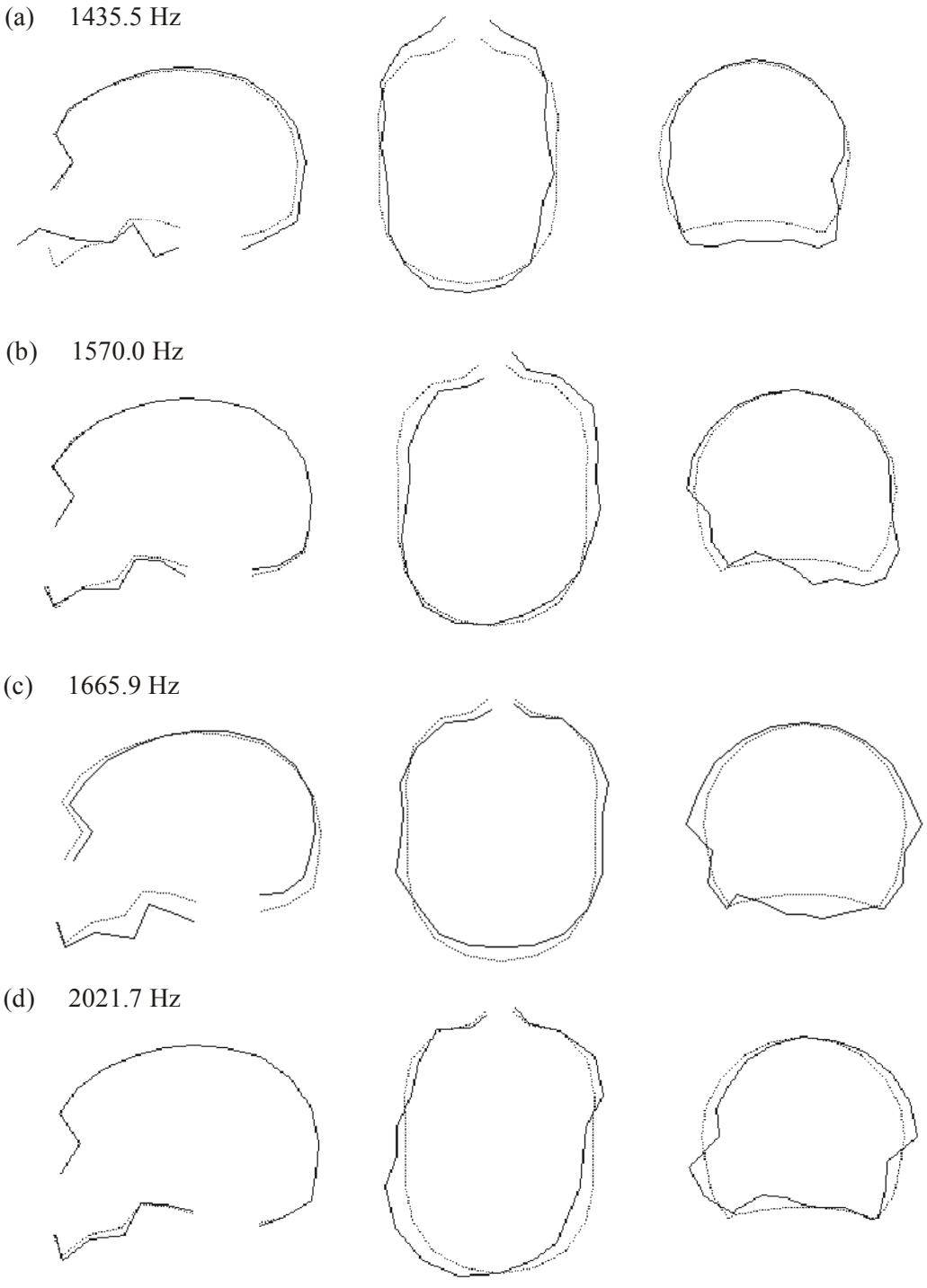

Fig.4: First four mode shapes of vibration of the dry skull (I).

female skulls were tested. However, the agreement between their measured fundamental natural frequency f_1=1385 Hz of the dry male skull and our results is very good.

The lowest resonant frequency of the human skull *in vivo* measurements was found out higher than 828 Hz by Hakansson et al. (1994) and the corresponding damping 8.9%, when patients with skin penetrating titanium implants in the temporal bone were investigated. Hakansson et al. (1996) also found that the human skull *in vivo* at normal hearing levels can be considered as a linear dynamic system, likewise in our study of the dry and non-dry skulls.

First four evaluated mode shapes of vibration for the lowest natural frequencies of the dry skull (I) are shown in Fig. 4. Even if the skull is not of a regular shape, the first and third mode shapes can be considered as symmetrical, and the second and forth modes as unsymmetrical related to the mid-saggital plane. The amplitudes of vibration in the lower part of the skull (the palate and the skull base) are dominant. There was no substantial difference between the dry skull (I) and (II) concerning the first two modes of vibration.

First two measured mode shapes of vibration of the non-dry skull were found to be similar to the modes for the dry skull.

Measured transfer functions between various anatomically significant points on the dry skull (I) and the STC point (surface of cochlea extremity of temporal bone) are shown in Fig. 5. The maximum vibration amplitude of the STC point is obtained by applying the excitation force at the point staphylion (*sta* – the hard palate edge). It might be important in a feedback mechanism for self-control of the speech.

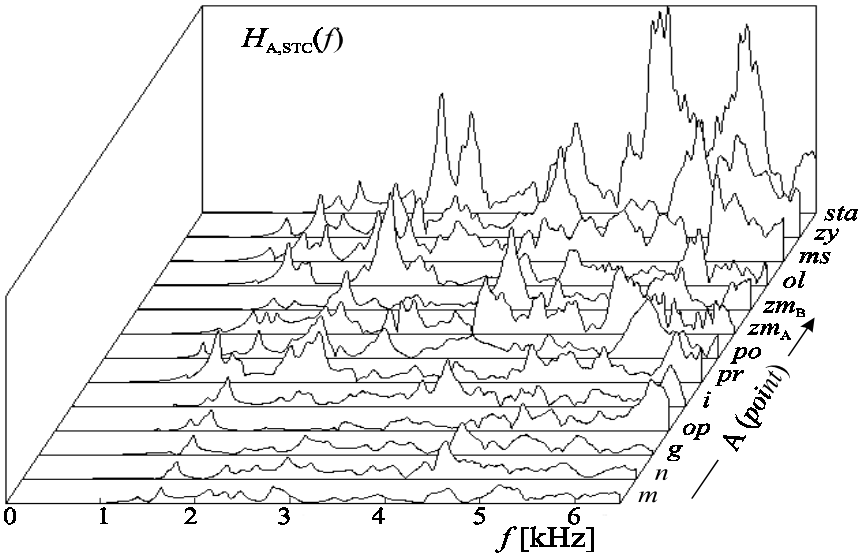

Fig. 5: Measured transfer functions at STC point exciting the dry skull at different points A.

In simplified theoretical considerations the skull can be considered as a thin-walled spherical shell structure. The lowest natural frequencies of the axisymmetric modes of vibration of a spherical shell are given by the formula (published, e.g. by Soedl,1981), which for the material properties of the skull (Voo et al., 1996): E_b=4.46.10^{9}Pa; μ_b=0.21; ρ_b=1410 kg/m^3 and for the geometry of the tested skull: $h \approx 5{,}4$ mm, $R \approx 95$ mm yields the lowest natural frequency f= 2245 Hz. This theoretical value can be used for a rough estimation of a frequency region expected as the most important in the vibration analysis of the skull. From the approximate formulas for a spherical shell it follows that for a smaller skull (lower R) the lowest natural frequency can be expected in a higher frequency range.

2.3. Measurement of the human head vibration *in vivo*

Several attempts to perform a reliable modal analysis of the human head on living subjects failed basically from the two following reasons.

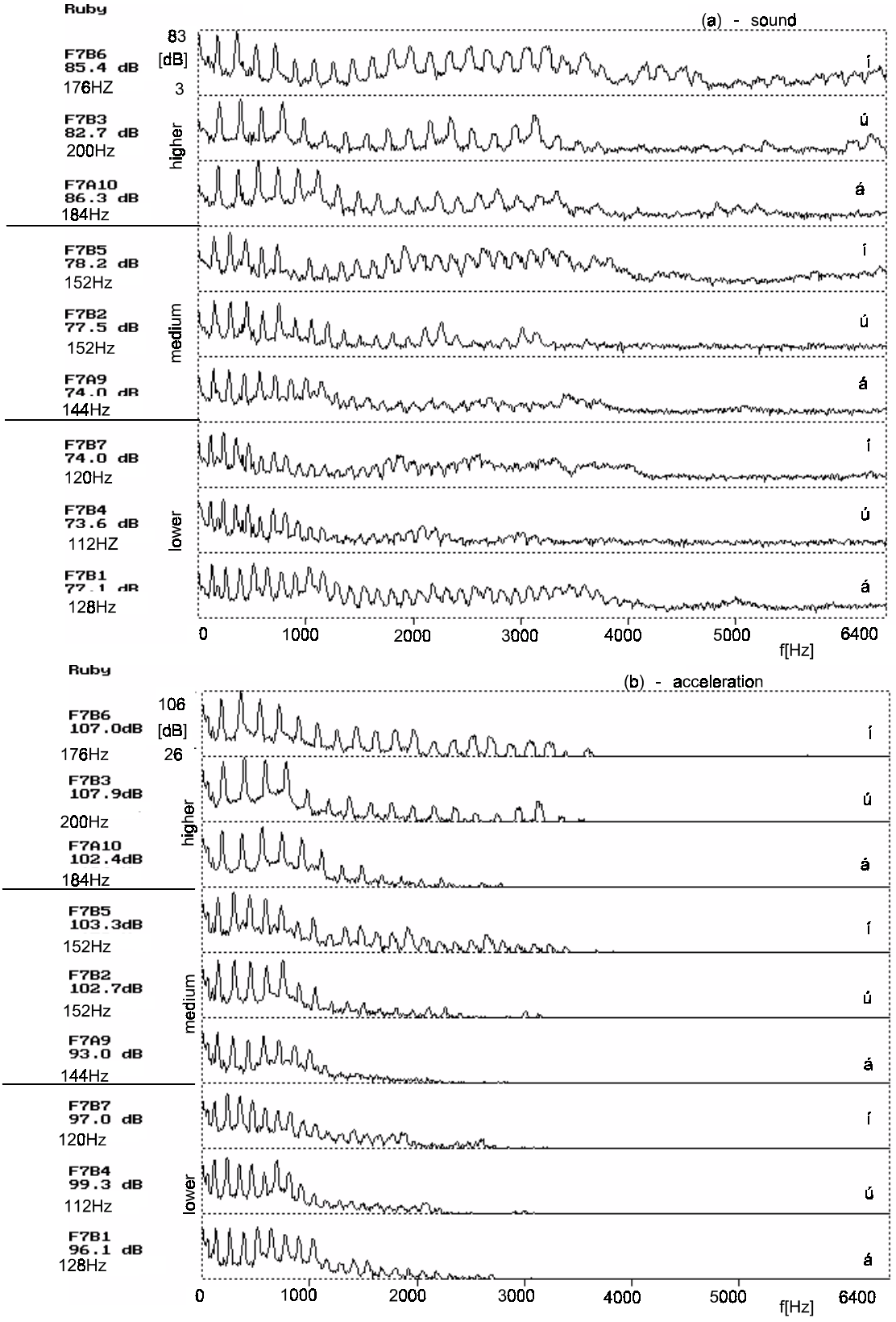

Fig. 6: Acoustic (a) and vibration (b) spectra for the singer's voice.

The first reason is that the energy needed for a defined and sufficient excitation of the head is extremely high comparing to the normal force level used in clinical practise, e.g., applying the bone vibrator.

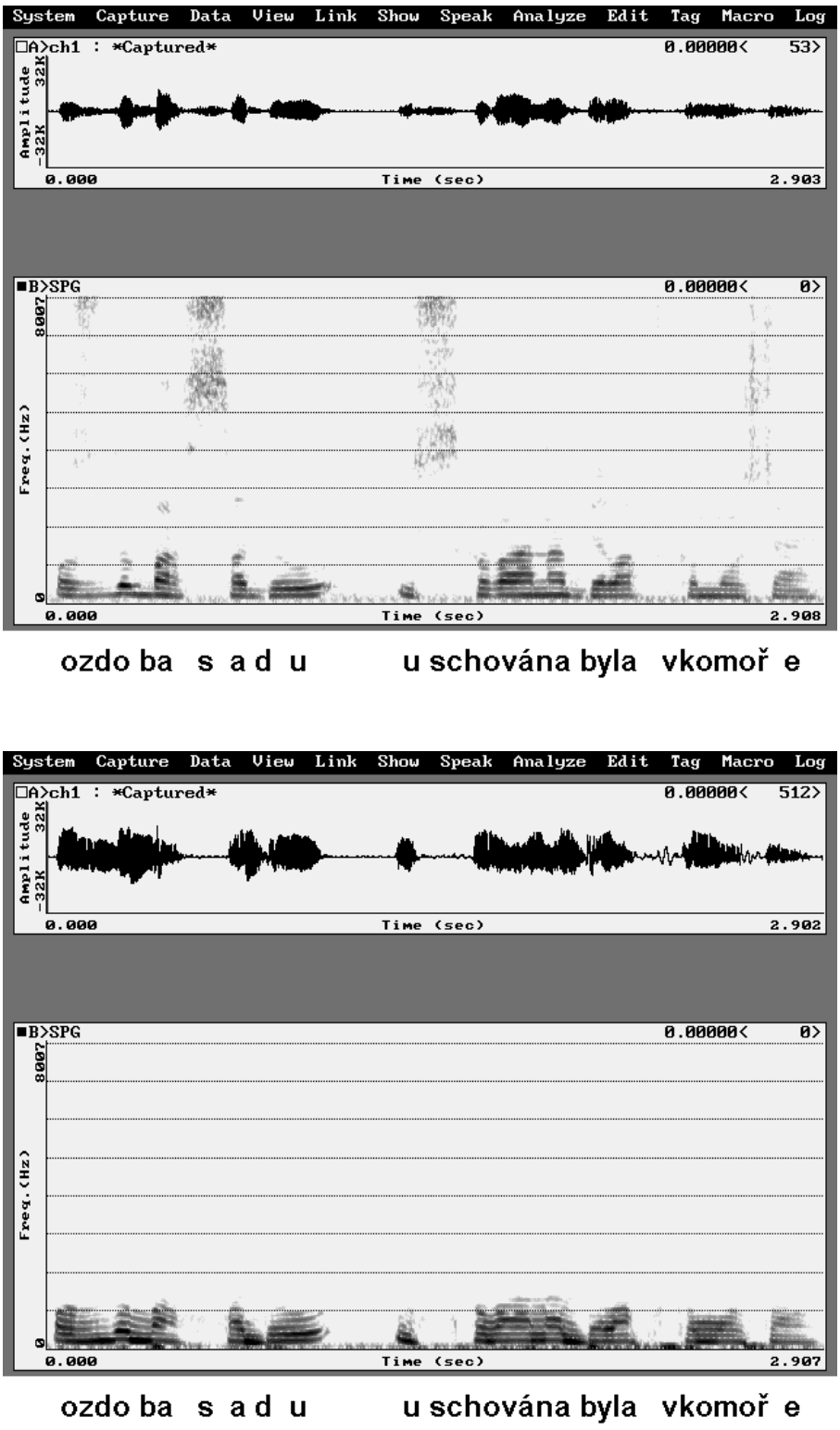

Fig. 7: Spectrograms of speech and head vibrations during a standard text reading.

The second problem is a proper fixing of the exciter to the head in order to minimize the energy losses in the transmission of the external excitation force into the skull bone through the skin. Intensive vibrations of the human head can be excited by the subject's own voice, even if we were not able to utilise this type of excitation for modal analysis.

The subject's voice was monitored by ½" B&K microphone in the distance of about 20 cm from the mouth and the vibration of the head was measured by B&K 4367 accelerometer slightly pressed by a rubber lent to the subject forehead.

Both the acoustic and the acceleration signals simultaneously measured were monitored by Dual Channel FFT Analyzer B&K 2032, recorded on the tape recorder and afterwards analysed using PC.

The subject's voice was monitored by ½" B&K microphone in the distance of about 20 cm from the mouth and the vibration of the head was measured by B&K 4367 accelerometer slightly

pressed by a rubber lent to the subject forehead. Both the acoustic and the acceleration simultaneously measured signals were on line analysed by Dual Channel FFT Analyzer B&K 2032, recorded on the tape recorder and afterwards analysed using PC.

Typical acoustic and vibration simultaneously measured spectra for a male singer are shown in Fig. 6 when singing the vowels /á, ú, í/, each of them for three different fundamental frequencies F0 (pitch) between 112-200 Hz and for the three different voice sound levels between 86-106 dB. The acoustic and vibration spectra are very similar up to the frequencies 2.5-3.5 kHz, and for the higher harmonics (frequencies n x F0 [Hz]) there are the identical maxima in the both spectra. The magnitude of the coherence function in these maxima was unity. It means that a linear relationship between the vibration level and the voice intensity exists. In a higher frequency range (f >3500 Hz) the vibrations of the head are much more damped than the sound signal.

Similar comparison of the acoustic signal and the acceleration of the speaker's forehead measured in the frequency range up to 8 kHz is demonstrated in the spectrograms in Fig. 7 when the subject was reading a standard text used in clinical investigations. While the sonogram in Fig. 7a contains the frequencies up to 8 kHz (see, e.g., consonant /s/) the spectrogram for vibrations in Fig. 7b contains noticeable frequencies only up to 2 kHz due to a much higher damping of higher frequencies. Nevertheless, the frequency region 0-2 kHz is sufficient for a good "understanding" of the voice signal recorded from the accelerometer and listen afterwards from the tape recorder.

3. Experimental transient analysis

Two contactless optical methods were used for investigation of the stress wave propagation in the skull after the impact: a) double pulse holointerferometry, b) the laserinterferometry.

3.1. Holointerferometry measurements

The measurement set-up for the double pulse holointerferometry is shown in Fig.8. The skull was freely positioned on a very soft rubber so that it was flexibly isolated from the holographic table.

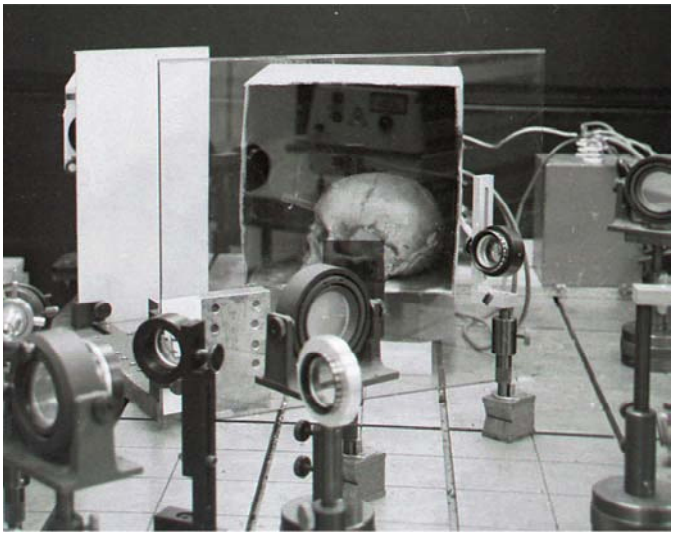

Fig.8: Holographic set-up used for recording interferograms of propagating waves.

The skull was dynamically loaded at the glabella (*g*) by impacts generated by exploding wires (Trnka et al., 1999, 2002). It enables to generate very short (15–25 ms) and intensive mechanical pulses (600–1700 N). The time history of the generated force is shown in Fig. 9. The excitation pulse covers the frequency range up to about 100 kHz.

The two ruby laser LUMONICS HLS2 light pulses were synchronised with the loading. The first laser pulse serves both for the pulse triggering of the electric circuit with the exploding wire and simultaneously for the holography record of the undeformed state of the skull. The second pulse is launched at any pre-set time variable from 1-800 ms.

The time of the beginning of the mechanical impact was delayed approximately 13 ms after the triggering pulse. The time delay includes the effects of the finite length of the loading element and the influence of parameters of the electric circuit.

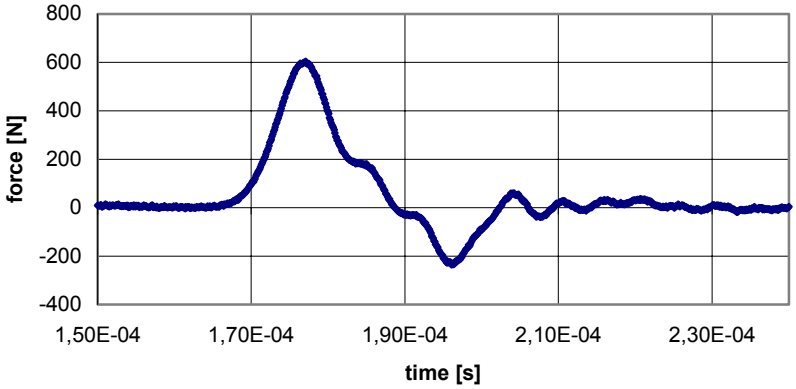

Fig.9: Impact force in time domain.

Holography records taken for the human dry and non-dry skull are compared in Fig. 10 for the time delay DT=60 ms between the two pulses of the laser. The propagating wave is visualized on the surface by black and white fringes that can be interpreted as the curves of constant amplitudes.

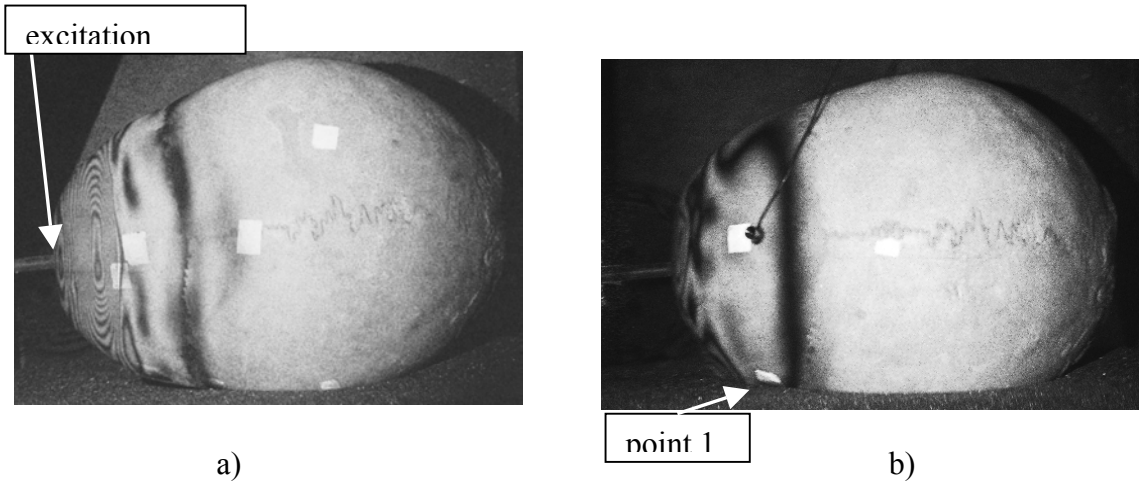

a) b)

Fig. 10: Holointerferograms recorded for the time delay DT=60 ms between the laser pulses for: a) dry skull, b) non-dry skull.

There is no substantial difference in the shape of the wave front propagating in the dry and non-dry skull. However, from the much higher density of the interference fringes for the dry skull it can be deduced that the wave amplitudes for the dry skull are much higher than for the non-dry skull. It is especially good visible near the point of the impact excitation. Comparing the position of the first black fringes it can be seen that the wave front in the non-dry skull propagates slowly than in the dry skull. Taking into account the time delay 13 μs the wave front velocities evaluated from the holointerferograms are approximately 2500 m/s for the dry skull and 2280 m/s for the non-dry skull.

3.2. Laserinterferometry measurements

Laser Vibrometer POLYTEC OFV 3000 was used for the measurements of the transient time velocity responses in several points on the skull, where a retroreflecting 3M foil strip was

glued on the bone (see, e.g. the point 1 in Fig. 10). The measurement of the velocity response was carried out simultaneously with the holointerferometry measurement. The velocity history was recorded on TEKTRONIX TDS 224 four channel digital oscilloscope and afterwards the data were transferred to PC.

Two time records of the measured velocities are shown in Fig. 11 for the dry and non-dry skull. The velocities were measured at the identical point on the dry and non-dry skull (at the point 1), and the time records exactly correspond to the holography measurements shown in Fig. 10.

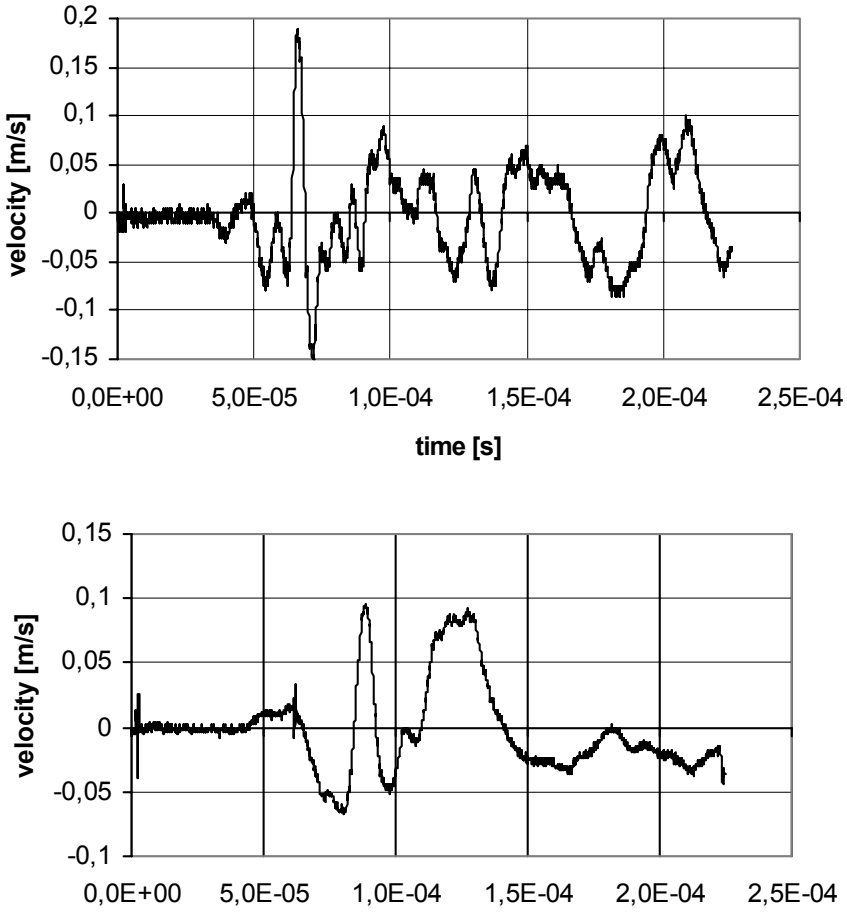

Fig.11: Velocity transient time responses measured at the point 1 (see Fig.10) on the dry (a) and non-dry (b) skull.

Comparing the results for the dry and non-dry skull it can be concluded that the maximum of the velocity response decreased due to the filling approximately into half, and that the filling damps more the higher frequencies. It can be also seen that the primary wave in the non-dry skull reaches the point 1 about 10 ms later than in the dry skull. Taking into account the above mentioned time delay correction $\Delta T \approx 13$ ms for the time records, the primary wave propagation velocity between 3500-3700 m/s for the dry skull and about 2500-2600 m/s for the non-dry skull can be estimated from Fig. 11. These values are higher than the wave propagation velocities evaluated from the holointerferograms in Fig. 10. The reason may be in a lesser distinguishability of the primary wave with very small amplitude in the holointerferograms, and subjectivity in evaluation of the measured data. Nevertheless the influence of the filling on the excited waves is significant; the waves propagating in non-dry skull are more damped and slower than the waves in the dry skull.

A relatively large scattering in the estimated wave propagation velocity is not caused only by the different measurement methods used and by subjectivity in the evaluation of holograms or time records. Substantial factors are also the differences in the way of impact generation and in the loading reproducibility (the input force is not directly measured in the experiment). Especially important are the force magnitude, loading direction and the frequency range involved in the force signal. A wide range of values (between 2500-4700 m/s) for the sound wave propagation velocities in human bones can be also found in literature

(Dreier & Com 1983). The other problem consists in an exact separation of different types of waves propagating in biocomposite shell structures.

4. Finite element modelling

4.1 FE model of the human skull for dynamical analysis

The developed FE model is based on the computer tomograph (CT) scanning of the male skull (II) investigated in the laboratory. The CT scan SIEMENS SOMATOM PLUS was used for taking the images. The basic bit data were transferred by FTP protocol to a PC and then each CT image was evaluated by a special algorithm for obtaining the outlines of the bone tissues. Afterwards the individual slices were composed by especially generated triangles to layers creating step by step the 3D model of the entire skull (Formánek, 1999). However, the model automatically created by the computer was too large for FE modelling some discontinuities and other types of inaccuracies were apparent in the model. Thus a special program was written to simplify the model and to create only inside and outside surface of each skull bone. Then using the pre-processor MENTAT of the FE code MARC the uneven surfaces were interactively smoothed and by manual regeneration of the mesh the number of elementary areas was reduced to 29 000. Due to the time consumption work only one half of the FE model of the skull was finished by this technique and the mid-saggital plane symmetry was introduced into the FE model for simplification. The complete FE model developed has 17 500 3D tetrahedral finite elements (see Fig. 12a).

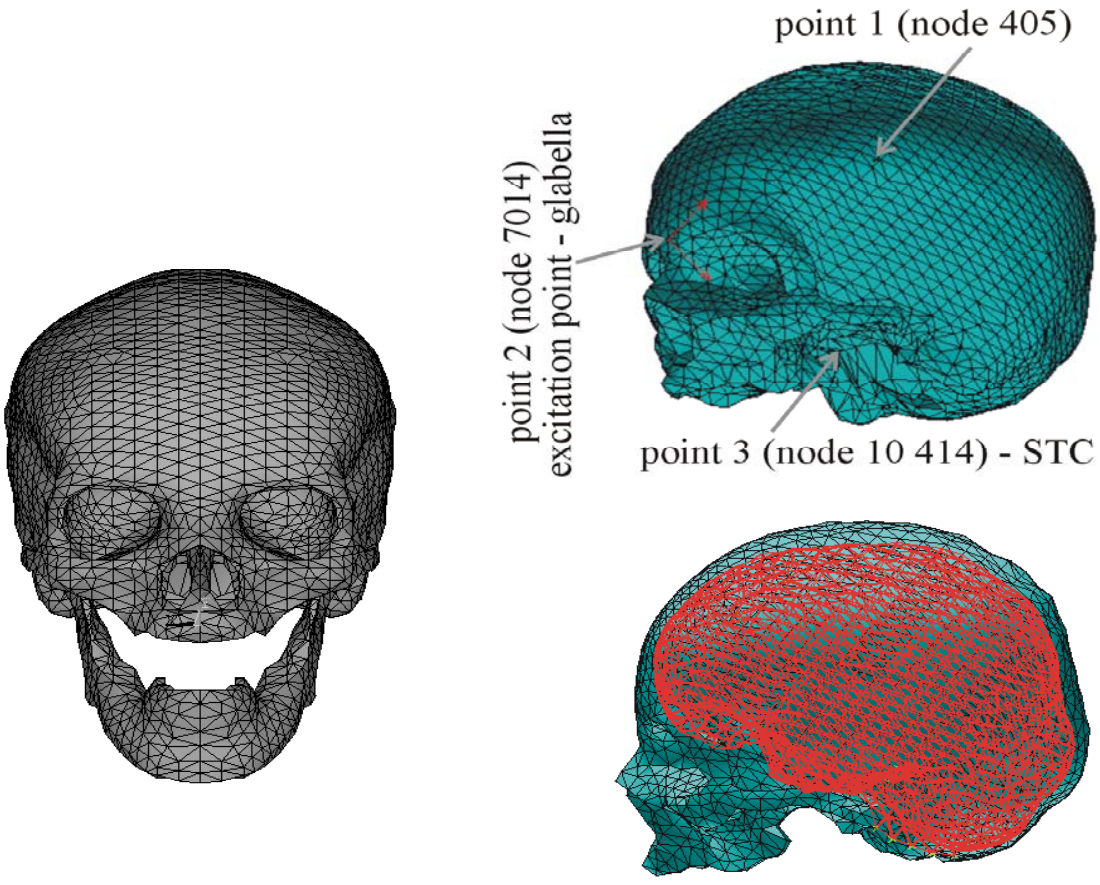

Fig. 12: FE model of the skull including the brain tissue.

The FE model of the dry skull without mandibula (Fig. 12b) consisted of 15 437 finite elements. The inner volume of the skull was automatically meshed by 30500 tetrahedral finite elements (Fig. 12c) and the complete FE model of the skull including the model of the brain consisted of 9311 nodes.

The following material properties were considered in the computations:

a) for the skull bones: Young's modulus $E_b = 4460$ MPa, mass density $\rho_b = 1410$ kg/m^3, Poisson's ratio $\mu_b = 0.21$.
b) for the filling: Young's modulus $E_f = 12\,000$ Pa, mass density $\rho_f = 1030$ kg/m^3, Poisson's ratio $\mu_f = 0.499999$.

On the interface between the skull bone and the filling simulating the brain tissue the all degrees of freedom of all common nodes were coupled.

4.2 Computational modal analysis

The modal analysis was performed using the FE code ANSYS and structural finite elements SOLID 72 with six degrees of freedom for each node. The eigenvalues and eigenvectors of the FE models were calculated by the reduced Hausholder method where as master degrees of freedom were used all degrees of freedom of all nodes on the bone-brain interface.

f_i [Hz]	1	2	3	4.	5	6	7	8
FEM	1442	-	1797	2223	2242	2389	-	2600
exp.	1388	1581	1776	2045	2261	2370	2438	2555
ε [%]	3,7	-	1,2	8	-0,9	0,8	-	1,7

Tab. 3: Computed and measured natural frequencies for the dry skull (II).

f_i [Hz]	1	2	3	4	5	6
FEM	1021	1102	1316	1409	1416	1510
exp.	1115	1243	1391	-	1576	-
ε [%]	-9,9	-9,7	-0,9	-	-8,3	-

Tab. 4: Computed and measured natural frequencies for the non-dry skull (II).

Computed fundamental natural frequencies are compared with the experimental values for the dry and non-dry skull (II) in Tabs. 3 and 4. The agreement between the calculated and measured lowest natural frequencies is reasonable; the differences are less than 10%. Some frequencies are missing in the theoretical results probably because the above-mentioned symmetry of the FE model is not satisfied for the real skull. Due to the dynamic added mass of the filling the first natural frequency of the skull theoretically decreased of about 30% comparing to the decrease 20% found in the experiment.

First two mode shapes of vibration computed for the dry and non-dry skull are shown in Fig. 13. The first modes are axisymmetrical with dominant vibration amplitudes at the skull base, especially at the hard palate. The second modes are antisymmetrical with the highest amplitudes at the temporal bones. In all cases the smallest amplitudes of vibration are at the forehead. Comparing the computed modes with the measured natural modes (see Fig. 4) it can be said that there is a relatively good qualitative agreement between the theory and the experiment. Similarly as in the experiment no substantial difference exists between the dry and wet mode shapes of vibration of the skull.

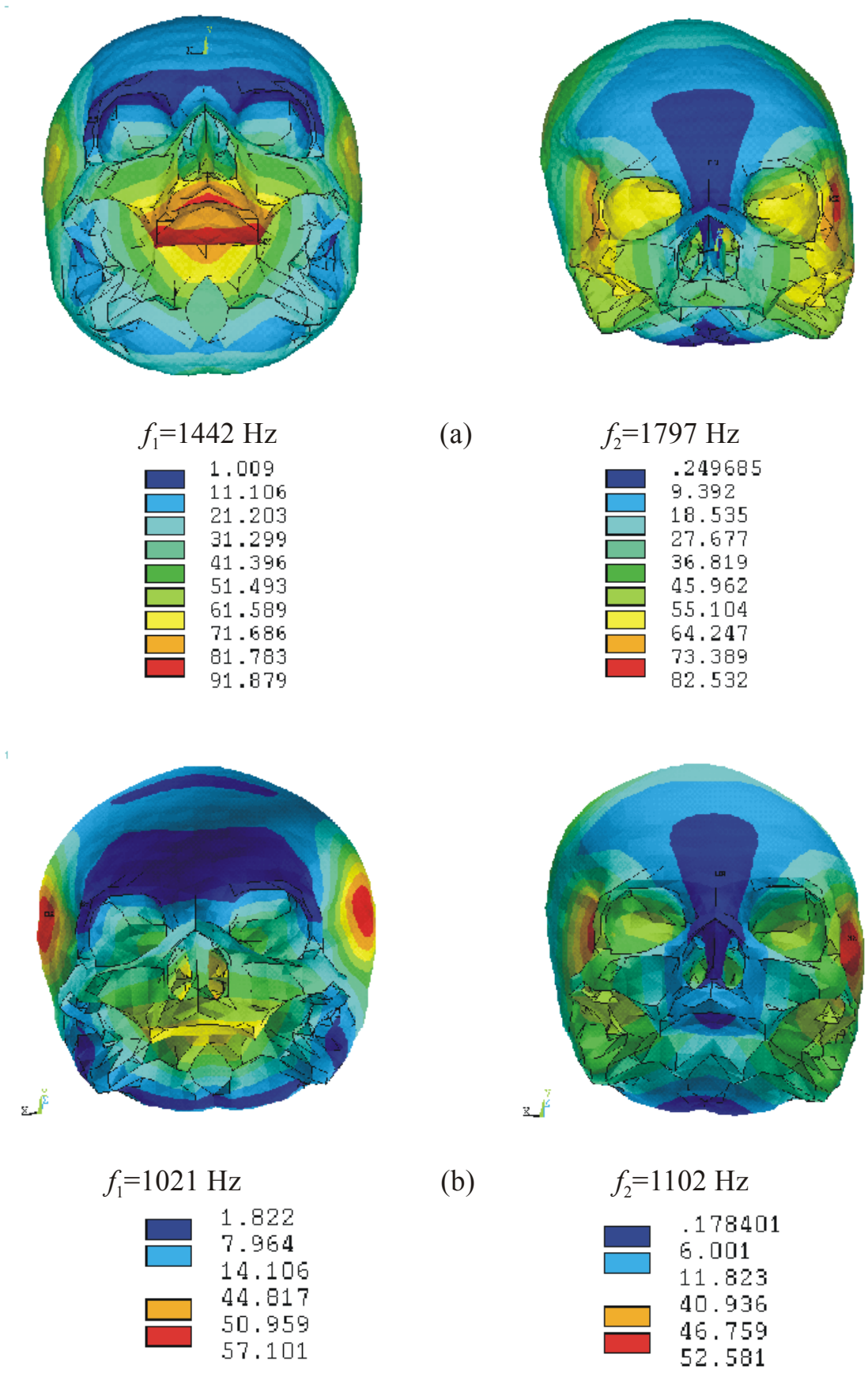

Fig. 13 First two computed mode shapes of vibration:
(a) for dry skull (II), for non-dry skull (II).

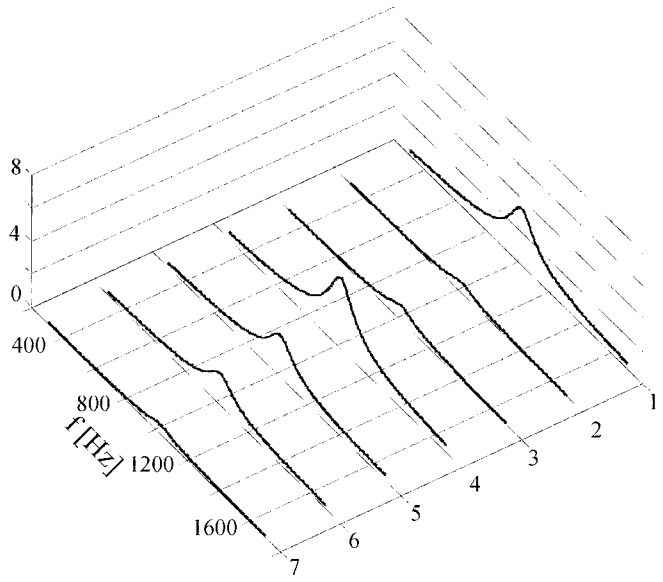

Fig. 14: Transfer functions calculated between various points on the non-dry skull and the point STC near cochlea: 1) *sta-STC*, 2) *zy-STC*, 3) *ms-STC,* 4) *ol-STC,* 5) *STC-STC,* 6) *op-STC,* 7) *m-STC*

4.3. Frequency response functions with simulation of brain tissue influence

The frequency dependent transfer functions between various anatomically important points on the skull were modelled using the developed FE model, where the simulation of the brain tissue was taken into account. Knowing the results of the modal analysis the transfer functions $h_{j,m}(\omega)$ between the jth and mth points were calculated by the superposition method:

$$h_{j,m}(\omega) = \sum_{k=1}^{N} x_{j,k}\left(i\omega - \lambda_k\right)^{-1} x_{k,m} + \sum_{k=1}^{N} \bar{x}_{j,k}\left(i\omega - \bar{\lambda}_k\right)^{-1} \bar{x}_{k,m}\,, \tag{1}$$

where N is the number of identified eigenmodes ${}^{T}\mathbf{x}_k = \left(x_{1\mathrm{k}}, \ldots x_{Mk}\right)$, $\lambda_k = -\sigma_k + i\omega_k$ is the kth eigenvalue, σ_k is the damping constant, ω_k is the eigenfrequency, and the horizontal line above the letters denotes complex conjugated values.
For the undamped system equation (1) yields the matrix of the transfer functions

$$\mathbf{h}(\omega) = \sum_{k=1}^{N} \frac{i\,2\omega_k \mathbf{x}_k{}^{T}\mathbf{x}_k}{\left(\omega_k^2 - \omega^2\right)}\,, \tag{2}$$

which for ortonormalised eigenvectors $\mathbf{y}_k$, related to the mass matrix, can be rewritten as

$$\mathbf{h}(\omega) = \sum_{k=1}^{N} \frac{\mathbf{y}_k{}^{T}\mathbf{y}_k}{\omega_k^2 - \omega^2}\,. \tag{3}$$

Comparison of the equations (2) and (3) gives:

$$\mathbf{x}_k = \frac{\mathbf{y}_k}{\sqrt{2i\omega_k}} \tag{4}$$

and substitution this equation to the equation (1) yields

$$h_{j,m}(\omega)=\sum_{k=1}^{N} y_{j,k}\left[2\omega_k\left(-\omega-(-i\sigma_k-\omega_k)\right)\right]^{-1} y_{k,m}+\sum_{k=1}^{N}-y_{j,k}\left[2\omega_k\left(-\omega-(-i\sigma_k+\omega_k)\right)\right]^{-1} y_{k,m}\,, \tag{5}$$

where the damping constants σ_k were determined from the damping ($D\approx0.07$) obtained by the experimental modal analysis.

The transfer functions, between the STC point near the cochlea and several anthropologically important points on the skull, computed in the frequency range 200-1600 Hz (Δf=8 Hz, N=6) in the direction of normal to the skull surface are shown in Fig. 14. Because the FE model is symmetrical, related to the mid-saggital plane, there are no resonant peaks in the transfer functions near the even eigenfrequencies, when the excitation point (e.g., *sta*, *ol*, *m*, *op*) is on the nodal line of the corresponding antisymmetrical mode. The dominant peaks in the dynamic response correspond to the first vibration mode with the resonant frequency 1021 Hz. The highest vibration amplitudes appear for the following configurations of the excitation point and the displacement at the STC point near cochlea: 1) *sta* – STC, 4) *ol*- STC and 5) STC – STC. It is in good qualitative agreement with the measurement of the transfer functions between the excitation force and the acceleration of the skull (see Fig. 5), where the highest sensitivity, related to the vibration level at the STC point, was found to be at the point *sta* at the end of the hard palate.

4.4 Numerical simulation of the transient time response after impact loading of the skull

Implicit Newmark integration method was used for calculation of the transient time response by the direct numerical integration of the equations of motion in the FE formulation within the ANSYS code. The computations were performed on the workstation DEC with the time step $\Delta t = 2.10^{-7}$ s. The force pulse in the time domain like in the experiments modeled the impact loading of the skull at the glabella (see point 2, node 7014 in Fig. 12).

The velocity time responses calculated in the normal direction to the surface of the skull bone in the point 1 (node 405 – see Fig. 12) are shown in Fig. 15 for dry and non-dry skull. The distance between the points of the impact excitation and the response (points 1 and 2) was Δl=8 cm. The symbols c_0, c_1, c_2 and c_R indicate the time delays, which correspond to the wave propagation velocities calculated from the data for the dry skull bones as follows:

a) dilatation wave in 1D continuum: $c_0 = \sqrt{E_b / \rho_b} = 1818$ m/s,

b) dilatation wave in 3D continuum: $c_1 = \sqrt{(\lambda_b + 2G_b) / \rho_b} = 1929$ m/s,
where λ_b is the Lame constant and G_b is the shear modulus for the bone,

c) shear wave in 1D continuum: $c_2 = \sqrt{G_b / \rho_b} = 1169$ m/s,

d) velocity of the Rayleigh surface wave: $c_R \cong 0.91\, c_2 = 1064$ m/s.

The wave propagation velocity 1852 m/s of the primary wave evaluated from Fig. 15 for the dry skull ($c=\Delta l/\Delta t\approx1852$ m/s, where $\Delta t\approx4.32.10^{-5}$ s) is close to the theoretical values c_1 or c_0 but this value is much less than the wave propagation velocities estimated from the holointerferometry and laserinterferometry measurements. Probably, the main reason is too small mesh density in the FE model. The model of the skull used for the calculations is not able to simulate the propagation of waves with high frequency components. An average size of one finite element in the FE model is of order about 7mm. Considering a minimum number of three finite elements per one wavelength needed for detection of this wave, it can be concluded that a maximum frequency for simulation of wave phenomena by this FE model is less than 85 kHz. However, the spectrum of the force excitation signal (see Fig.9) contains frequencies higher than 100 kHz.

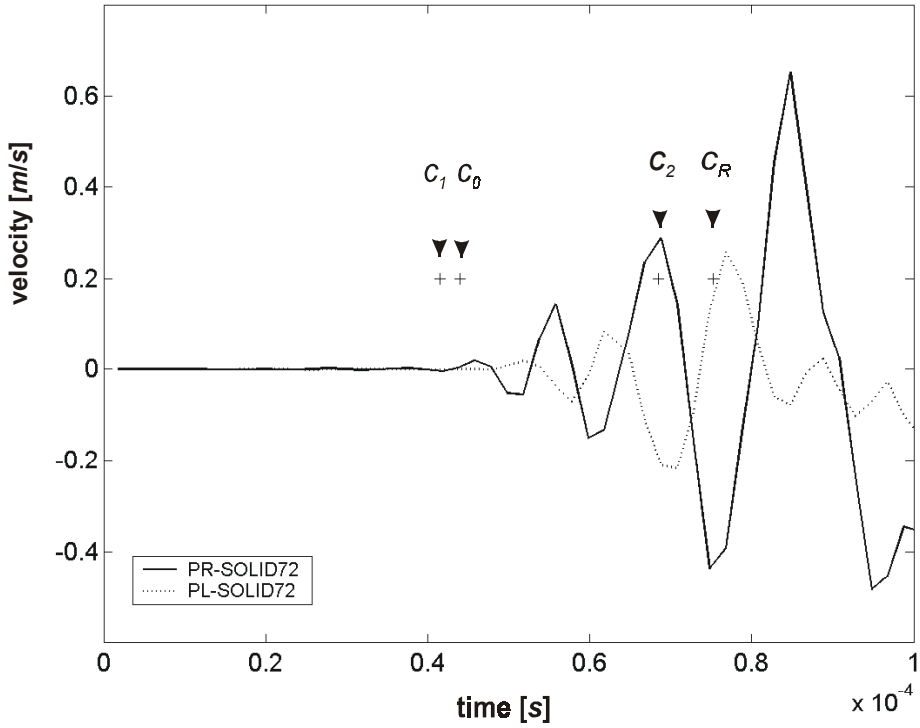

Fig. 15: Velocity time responses calculated in the point 1 (node 405) on the dry (full line) and non-dry (dotted line) skull after impact loading at the point 2 (*g*-glabella, node 7014); symbols c_1, c_0, c_2, c_R denote time delays for classical wave velocities.

The primary wave estimated from Fig. 15 for the non-dry skull with the filling is delayed of about 5μs behind the wave for the dry skull. The wave propagation velocity evaluated for the non-dry skull is $c \approx 1660$ m/s (for $\Delta t \approx 4.82.10^{-5}$ s), and the maximum of the deformation velocity in the time response is nearly three times less than for the dry skull. Consequently the influence of the filling is to attenuate and to slow down the waves propagating in the skull. No material damping was considered in the calculations.

Similar conclusion follows from Fig. 16 where the displacements of skull surface are shown in time t=60μs after the impact. Comparing the results for the dry and non-dry skull a qualitative conformity of the displacement counter lines in both cases can be seen; however, the deformation wave propagates in the non-dry skull with smaller amplitudes and with smaller velocity of the primary wave.

5. Comments, remarks and discussion of the results

Acceptable agreement between the computed and measured natural frequencies and fundamental mode shapes of vibration of the skull was obtained. The agreement of the presented results with the experimental study of Khalil et al (1979) is very good. The natural frequencies of the tested dry skulls were found to be higher than approximately 1400 Hz, and the damping 1–2%. Our results for the skull filled by the gelatine are in good agreement with the study by Hakansson et al. (1994), where the lowest resonant frequency of the human skull *in vivo* was found in the range from 828-1164 Hz and the corresponding damping 9%.Decrease of the fundamental natural frequencies due to the added mass of the gelatine was

substantial as well as the increase of the damping due to its viscosity. Mode shapes of vibration of the dry and non-dry skull are similar.

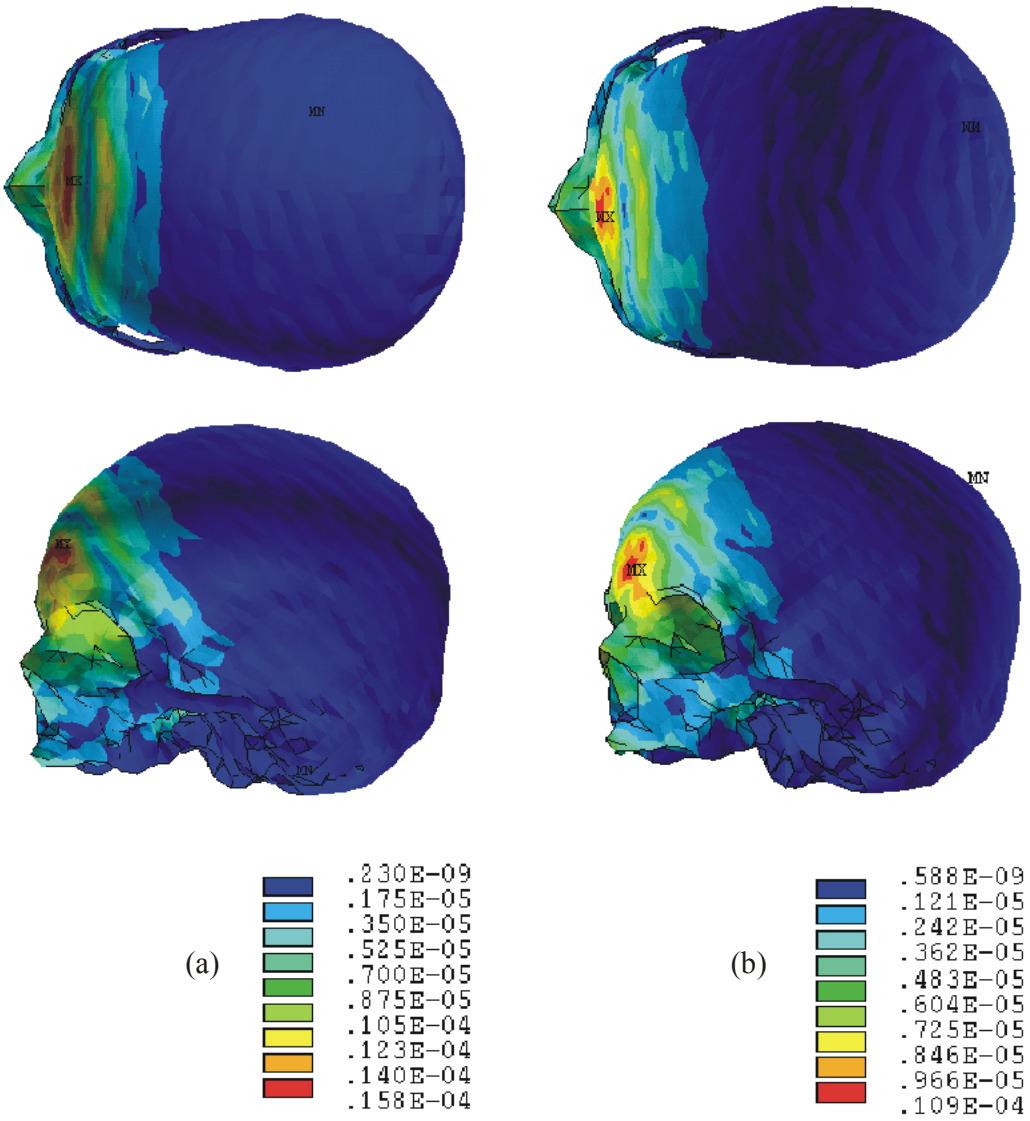

Fig. 16: Displacement response calculated in time t=60 ms after impact loading the skull at glabella (point 2, node 7014): a) dry skull, b) non-dry skull.

Interesting is that the most sensitivity place to the vibration excitation of the skull near cochlea (STC point) was found to be at the hard palate edge. This experimental result for the dry skull was confirmed by the computations of the frequency dependent transfer functions for the FE model of the non-dry skull. Vibration of the skull base including the hard palate was found substantial for most of the natural frequencies. Consequently the transmission of the voice from the vocal tract to the cochlea and to the brain may be important in the frequency regions where the dominant resonant frequencies exist.

High coherence of the forehead vibrations and own subject voice was found in the frequency region up to 2 kHz. However, in agreement with the studies by Mišun & Přikryl (2001), where the role of the resonances of the skull bones for the sound transfer outside or

inside the skull was found negligible, no resonant frequencies of the human head were detected in the vibration spectra. This is probably caused by a high damping of the skull bone structure by the soft tissues. A feeling of singers that they can amplify their voice sound level by a resonance of the skull seems to be subjective, and it might be evoked by an internal soft tissue resonance.

Calculation of the transient time response of the dry skull by direct Newmark integration of equations of motion with hundreds of time steps needs several hours of computation time of the DEC workstation and several times more for the non-dry skull. For a finer FE meshing the demands on the computer memory and computational time are increasing very rapidly. Thus the accuracy of the results is restricted by the wave dispersion in higher frequency region due to an insufficient spatial discretization in the FE model. A course mesh in the FE model of the skull limited the numerical calculations only up to about 85 kHz that was lower value than the frequency components higher than 100 kHz in the spectrum of the impact force used in the experiments. Comparison of the results of the FE modelling with the experiments is also influenced by an exact correct modelling of the real material properties of the system (e.g., the wet filling causes undefined changes of the material properties of the skull bones, and the material parameters of the filling are not strictly determined including the uncertainty in the preparation process).

6. Conclusion

The qualitative agreement between the results of the FE modelling and the experiments is reasonable from above mentioned point of view. The developed FE model is promising to simulate reasonably the fundamental dynamical properties of the skull. The model can be used in an audible frequency range (10-16 kHz) for numerical simulation of the sound transmission in the skull by the bone conduction to the inner ear. Both the theoretical and experimental results showed substantial attenuation of the amplitudes of the waves propagating in the skull when the model of the brain tissue was taken into account. Similarly, due to the interaction of the skull bones and the soft brain tissue, modelled by the gelatine, the stress wave propagation velocity in the skull is substantially reduced, according to the experimental results to about 70% and simultaneously the wave amplitudes decreased approximately into half.

7. Acknowledgements

The study was supported by the project of the Grant Agency of the Czech Republic No 106/98/K019: Methods of Mathematical-Physical Modelling of Vibroacoustic Systems in Biomechanics of Voice and Hearing, and the holointerferometry investigations also by the project of the Grant Agency of the Czech Academy of Sciences No A2076904: Diagnostic of Transient Dynamic Responses in Plate and Shell Structures.

References

Bandak F. A.: On the mechanics of impact neurotrauma: A review and critical synthesis, J. of Neurotrauma, 12, (4) (1995) 635-649.

Daněk, O., Kozánek, J.: Mathematical models of dynamic systems with general structure, Strojnícky časopis, 49 (2) (1998) 81-96 (in Czech).

Durrant J. D., Hyre R.: Observations on temporal aspects of bone-conduction clicks: Real head measurements, J. Am. Audiol. 4 (1993) 213-219.

Formánek P.: Development of the FE models of parts of human body from CT scanning, In: Proc. of the Conf. Engineering Mechanics'99, 17-20 May 1999, Svratka, pp. 503-508 (in Czech).

Hakansson B., Brandt A. & Carlsson P.: Resonance frequencies of the human skull in vivo, J. Acoust. Soc. Am. 95 (1994) 1474-1481.

Hakansson B., Carlsson P., Brandt A. & Stenfelt S.: Linearity of sound transmission through the human skull in vivo, J. Acoust. Soc. Am. 99 (1996) 2239-2243.

Horáček, J., Formánek, P., Hendrych, P., Pešek, L.: FE model of the human skull for dynamic analysis, In: Proc. of Conf. Biomechanika člověka 2000, 24.-25.11.2000, Olomouc, pp. 45-48

Hoyer H.E. & Dörheide J.: A study of human head vibrations using time-averaged holography. J. of Neurosurgery 58 (1983) 729-733.

Khalil T. B., Viano D. C. and Smith D. L.: Experimental analysis of the vibrational characteristics of the human skull. J. of Sound and Vibration 63 (1979) 351-376.

King A.I., Ruan J.S., Zhou C., Hardy W.H., and Khalil T. B.: Recent advances in biomechanics of brain injury research: A Review, J. of Neurotrauma 12 (4) (1995) 651-658.

Kozánek J.: Smoothing identification method of transfer functions, In: Proc. of the Ninth World Congress on the Theory of Machines and Mechanisms, Politecnico di Milano, 29 Aug.-2 Sept. 1995 vol. 2, pp. 1425-1429.

Krabbel G., Appel H.: Development of a FE model of the human skull, J. of Neurotrauma 12 (4) (1995), 735-742

Kršek P.: Possibilities of creation of FEM models from CT/MR data, In: Proc. of Conf. Engineering Mechanics. Svratka, 15.-18. 5. 2000, pp. 27-32 (ISBN 80-86246-06-X).

Kuijpers A.H., Claessens M. H., Sauren A. A.: The influence of different boundary conditions on the response of the head to impact - a 2D FE study, J. of Neurotrauma 12 (4) (1995) 715-724.

Kumaresan S., Radhakrishnan S.: Importance of partitioning membranes of the brain and the influence of the neck in head injury modelling, Medical & Biological Engineering Computing 34 (1996) 27-32.

Laitakari K., Löppönen H.: Monitoring bone conduction hearing aids in situ, Rev. Laryngol. Otol. Rhinol. 116 (4) (1995) 305-307.

Mišun V, Přikryl K: The analysis of the human voice spreading through the inner skull path toward the hearing system, In: Proc. of Inter. Conf. MEDICON 2001, 14-15 June 2001, Pula, Croatia, 2001, 4 pages.

Ogura Y., Masuda Y., Miki M., Takeda T., Watanabe S. and Ogawara T.: Vibration analysis of the human skull and auditory ossicles by holographic interferometry, In: G. von Bally (ed.): Holography in Medicine and Biology, Springer Verlag, Berlin, 1979.

Pawlowski, Z., Pawloczyk, R., and Kraska, Z.: Epiphysis vibrations of singers studied by holographic interferometry, In: A. Askenfelt, S. Felicetti, E. Jansson, & J. Sundberg (Eds.), Proc. of the Stockholm Music Acoustics Conf. 1983 (SMAC 83). Stockholm: Royal Swedish Academy of Music, 1985, 37-60.

Pešek L., Horáček J., Hendrych P.: Numerical modeling and modal analysis of human skull with simulation of brain tissue, In: Proc. of Interaction and Feedbacks 2000, IT AS CR, Prague, 28.-29. 11. 2000, pp. 173-176 (ISBN 80-85918-58-7) (in Czech)

Přikryl, K.: Analysis of bone conducted acoustic energy by the human crania, In: Proc. of Engineering Mechanics 2001, May 14-17, 2001, Svratka, pp. 229-230 (in Czech).

Dreier, N., Com, B.: Diagnostic Ultrasound, Bruel & Kjaer, 1983.

Soedel W.: Vibrations of shells and plates, Marcel Dekker, INC., New York, 1981.

Stenfelt S., Hakansson B.: Vibration characteristics of bone conducted sound in vitro, J. Acoust. Soc. Am. 107 (1) (2000) 422-431.

Sundberg J.: To perceive one´s own voice and another person´s voice. In.: Research aspects on singing, Royal Swedish Academy of Music Stockholm, (33) (1981) 80-96.

Sundberg, J.: Phonatory vibrations in singers: A critical review, Music Perception, The Regents of the University of California, 9 (3), (1992) 361-382.

Trnka, J.: Holointerferometry investigation of resonance modes of vibration of a skull. In: Proc. of Colloq. Dynamics of Machines'99, IT AS CR, Prague, 9.-10.2.1999, pp. 263-266 (in Czech).

Trnka, J. and Veselý, E.: Impact loading in experimental investigation of stress waves propagation in plates and shells, In: Proc. of Engineering Mechanics'99, 13.-20.5. 1999, Svratka, pp.469-474 (in Czech).

Trnka J., Landa M., Dvořáková P.: Dynamic responses of plate and shell structures studied by nondestructive testing method, 40th Int. Conf. Experimental Stress Analysis EAN, 3.-6. VI. 2002, Prague, pp. 253-259.

Voo K., Kumaresan S., Pintar F.A.: Finite - element models of the human head, Medical & Biological Engineering Computing 34 (1996) 375-381